Inorganic Chemistry

Article

pubs.acs.org/IC

Synthesis and Characterization of [Ir(1,5-Cyclooctadiene)(μ-H)]$_4$: A Tetrametallic Ir_4H_4-Core, Coordinatively Unsaturated Cluster

Kuang-Hway Yih,[†] Isil K. Hamdemir,[‡] Joseph E. Mondloch,[‡] Ercan Bayram,[‡] Saim Özkar,[§] Relja Vasić,[⊥] Anatoly I. Frenkel,[⊥] Oren P. Anderson,[‡] and Richard G. Finke*[,‡]

[†]Department of Applied Cosmetology, Hungkuang University, Taichung, Taiwan 433

[‡]Department of Chemistry, Colorado State University, Fort Collins, Colorado 80523, United States

[§]Department of Chemistry, Middle East Technical University, 06531 Ankara, Turkey

[⊥]Department of Physics, Yeshiva University, New York, New York 10016, United States

Supporting Information

ABSTRACT: Reported herein is the synthesis of the previously unknown [Ir(1,5-COD)(μ-H)]$_4$ (where 1,5-COD = 1,5-cyclooctadiene), from commercially available [Ir(1,5-COD)Cl]$_2$ and $LiBEt_3H$ *in the presence of excess 1,5-COD* in 78% initial, and 55% recrystallized, yield plus its unequivocal characterization via single-crystal X-ray diffraction (XRD), X-ray absorption fine structure (XAFS) spectroscopy, electrospray/atmospheric pressure chemical ionization mass spectrometry (ESI-MS), and UV−vis, IR, and nuclear magnetic resonance (NMR) spectroscopies. The resultant product parallels—but the successful synthesis is different from, vide infra—that of the known and valuable Rh congener precatalyst and synthon, [Rh(1,5-COD)(μ-H)]$_4$. Extensive characterization reveals that a black crystal of [Ir(1,5-COD)(μ-H)]$_4$ is composed of a distorted tetrahedral, D_{2d} symmetry Ir_4 core with two long [2.90728(17) and 2.91138(17) Å] and four short Ir−Ir [2.78680 (12)−2.78798(12) Å] bond distances. One 1,5-COD and two edge-bridging hydrides are bound to each Ir atom; the Ir−H−Ir span the shorter Ir−Ir bond distances. XAFS provides excellent agreement with the XRD-obtained Ir_4-core structure, results which provide both considerable confidence in the XAFS methodology and set the stage for future XAFS in applications employing this Ir_4H_4 and related tetranuclear clusters. The [Ir(1,5-COD)(μ-H)]$_4$ complex is of interest for at least five reasons, as detailed in the Conclusions section.

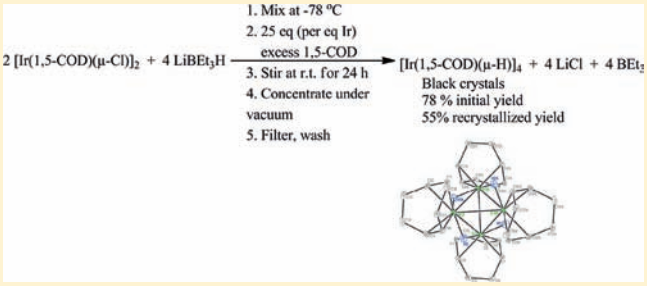

INTRODUCTION

Molecular metal clusters[1] containing four metal atoms, M_4, are an interesting, increasingly important, and evolving area of inorganic, organometallic, catalytic, and related sciences. Tetrametallic clusters of Ru, Os, Rh, or Ir have been synthesized, fully characterized, and used as precatalysts for the catalytic hydrogenation of alkenes, arenes, CO, aldehydes, and ketones as well as in hydroformylation, cyclooligomerization, cyclization, and polymerization reactions.[2] Known tetrametallic complexes of group 9 metals including Rh, Ir, and Co, and which contain a [M(μ-H)]$_4$ core, include [Rh(1,5-COD)(μ-H)]$_4$ (where 1,5-COD = 1,5-cyclooctadiene),[3] [Ir(CO)(μ-H)H(PPh_3)]$_4$,[4] [Ir(η^5-C_5Me_5)(μ-H)]$_4$(BF_4)$_2$,[5] [Co(η^5-C_5H_5)(μ-H)]$_4$,[6] and [Co(η^5-C_5Me_4Et)(μ-H)]$_4$.[7]

From the above known [M(μ-H)]$_4$-core complexes, the tetrarhodium complex [Rh(1,5-COD)(μ-H)]$_4$ is particularly relevant to the present work. This [Rh(1,5-COD)(μ-H)]$_4$ complex was first synthesized by Muetterties and co-workers starting with the commercially available [Rh(1,5-COD)(μ-Cl)]$_2$ complex and K[HB(O-*i*-Pr)$_3$], as detailed in Scheme 1.[3]

A single-crystal structural investigation revealed the Rh_4 core, with two long and four short Rh−Rh distances. In that publication, hydrides were located using difference Fourier techniques between two Rh atoms connected by short Rh−Rh distances.[3] The assignment of four short bonds to the Rh−H−Rh groups is consistent in a general way with the prior literature.[8] [Rh(1,5-COD)(μ-H)]$_4$ proved to be a good precatalyst for hydrogenation of toluene in cyclohexane-d_{12}[9] and hydrogenation of carbon dioxide.[9] The active catalyst species is believed to be Rh metal under toluene hydrogenation conditions. Kinetic studies performed on a catalytic carbon dioxide hydrogenation system suggested a neutral rhodium(I) hydride species ([Rh(H)($Ph_2P(CH_2)_4PPh_2$)]$_x$, where x = 1 or 2−4) as the active catalyst.[9c]

Somewhat surprisingly, the Ir analogue of the above Rh complex, [Ir(1,5-COD)(μ-H)]$_4$, has not been previously described, most likely because attempted syntheses, analogous to that of the Rh congener, *fail* (yields ≤ 1%, vide infra). The 56-total-electron [Ir(1,5-COD)(μ-H)]$_4$ complex has a formal 17 electron count at each Ir and thus is coordinatively unsaturated.

Received: December 8, 2011
Published: February 22, 2012

   dx.doi.org/10.1021/ic2026494 | *Inorg. Chem.* 2012, 51, 3186−3193

Scheme 1. Balanced Reaction Stoichiometry and the Reaction Conditions for the Synthesis of $[Rh(1,5\text{-COD})(\mu\text{-H})]_4$ (Adapted from Reference 3a)

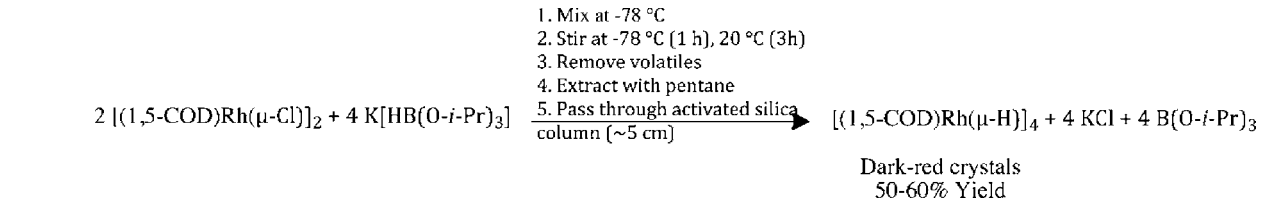

Our recent work on Ir-based models of a Ziegler-type industrial hydrogenation catalyst prepared from $[Ir(1,5\text{-COD})(\mu\text{-}O_2C_8H_{15})]_2$ plus $AlEt_3$ revealed that Ir_4 species are a dominant, initial form of the Ir present.[10] Hence, $[Ir(1,5\text{-COD})(\mu\text{-H})]_4$ with its Ir_4H_4 core (vide infra) is of interest as a new precursor for testing the formation and stabilization mechanisms of such Ziegler-type hydrogenation catalysts.[10,11] More specifically, the new complex $[Ir(1,5\text{-COD})(\mu\text{-H})]_4$ is of value as a fully compositionally and structurally characterized Ir_4 analogue of the, on average, Co_4-based, subnanometer clusters identified by X-ray absorption fine structure (XAFS) spectroscopy as a dominant species in Co-based Ziegler-type industrial hydrogenation catalysts. Such Ziegler-type industrial hydrogenation catalysts[12] are used industrially to produce styrenic block copolymers at a level of $\sim 1.7 \times 10^5$ metric tons/year.[13] In addition, $[Ir(1,5\text{-COD})(\mu\text{-H})]_4$ is of considerable interest as a possible Ir−H-containing, tetrametallic Ir_4H_4 intermediate in the nucleation and growth of Ir^0_n nanoclusters starting with $(COD)Ir^+$ precatalysts[14] and with stabilizers such as $[P_2W_{15}Nb_3O_{62}]^{9-}$, HPO_4^{2-}, and $AlEt_3$.[10,11,12,15] Whether or not such polynuclear metal hydride $(M-H)_n$ species are key intermediates in M^0_n nanoparticle formation—rather than the presently assumed M^0 intermediates—remains controversial. The availability of precatalysts and possible intermediates derivable from $[Ir(1,5\text{-COD})(\mu\text{-H})]_4$ opens up the possibility of QEXAFS and other direct-method tests with such discrete, fully characterized, Ir_4H_4-core complexes.[14]

Herein, we report (i) the 78% initial, and 55% recrystallized, yield synthesis of the previously unknown $[Ir(1,5\text{-COD})(\mu\text{-H})]_4$ starting from commercially available precursor $[Ir(1,5\text{-COD})(\mu\text{-Cl})]_2$ and $LiBEt_3H$ in which *added, excess 1,5-COD* is one key to the improved yield (vs <1% by the literature routes for the Rh congener, vide infra), and then (ii) the complete characterization of the resultant pure, crystalline product by single-crystal X-ray diffraction (XRD), XAFS, electrospray/atmospheric pressure chemical ionization mass spectrometry (ESI-MS), UV−vis, IR, and NMR. There are at least five reasons (a couple of which are given above) as to why the present complex is of interest, a full list of which is given as part of the Summary and Possible Future Directions section.

EXPERIMENTAL SECTION

Materials. All manipulations were performed under N_2 in a Vacuum Atmospheres drybox (≤5 ppm O_2 as monitored by a Vacuum Atmospheres O_2-level monitor) or, where noted, using a Schlenk line. All glassware was dried overnight in an oven at 160 °C, cooled under vacuum in a desiccator, and then transferred into the drybox while still in the desiccator and under vacuum. $[Ir(1,5\text{-COD})(\mu\text{-Cl})]_2$ (an orange powder, Strem Chemicals, 99%), $LiBEt_3H$ [as a colorless solution in 1.0 M tetrahydrofuran (THF), Aldrich], toluene (Aldrich, 99.8%, anhydrous), and benzene-d_6 [Cambridge Isotope Laboratories, Inc., 99.5%, w/o tetramethylsilane (TMS)] were used as received. THF (Mallinckrodt Chemicals AR ACS, 500 mL), *n*-hexane (Sigma-Aldrich, Reagent Plus, ≥99%, 500 mL), and cyclohexane (Sigma-Aldrich, 99.5%, H_2O < 0.001%) were distilled over sodium/benzophenone under N_2(g) and transferred into the drybox under air-free conditions. Acetone (Burdick and Jackson, >99.9% purity, 0.44% water) and H_2O (Nanopure ultrapure H_2O system, D4754) were degassed by connecting to a Schlenk line and then passing Ar for 5 min through the solution.

Synthesis of $[Ir(1,5\text{-COD})(\mu\text{-H})]_4$. In the drybox, the orange powdered $[Ir(1,5\text{-COD})(\mu\text{-Cl})]_2$ (1.3434 g, 2 mmol) was weighed out and then transferred into a 100 mL round-bottomed Schlenk flask equipped with a side arm and a $^5/_8 \times {}^5/_{16}$ in. Teflon-coated magnetic stirbar. The flask was sealed, removed from the drybox, and placed on a Schlenk line under Ar via its side arm. Next, 70 mL of room temperature THF was added to the flask using a cannula, forming an orange solution with some undissolved orange powder. The flask containing the orange solution of $[Ir(1,5\text{-COD})(\mu\text{-Cl})]_2$ was placed in an acetone/dry ice bath at −78 °C and stirred for 15 min. A 2.5 mL gastight syringe was purged three times with Ar using a Schlenk line and then used to measure out 4 mL (4 mmol) of $LiBEt_3H$. $LiBEt_3H$ was then added dropwise to the orange $[Ir(1,5\text{-COD})(\mu\text{-Cl})]_2$ solution under an Ar atmosphere with vigorous stirring. The original orange color of the solution changed to dark brown upon the dropwise addition of $LiBEt_3H$. The resulting solution was stirred at −78 °C for an additional 10 min and then warmed to room temperature. The solution slowly turned from dark brown to dark green within 10 min of additional stirring at room temperature. 1,5-COD (12.3 mL, 25 equiv per Ir) was measured out with a 20 mL gastight syringe purged with Ar and then added over 5−10 min to the dark-green solution. The resulting bright-green solution was stirred at room temperature for 24 h and then concentrated to ~5 mL under vacuum at room temperature using a Schlenk line. A visually apparent black powder was formed in the bright-green solution. The black powder was separated from the bright-green solution under Ar using a Schlenk-ware medium-porosity glass frit of ca. 16 μm pore size. The open end of the Schlenk glass frit was sealed by a rubber septum. The black powder collected on top of the glass frit was washed with degassed H_2O (5 mL × 2) and then degassed acetone (5 mL × 3) using a gastight syringe that was previously purged with Ar. The black powder was then dried overnight under vacuum at room temperature, resulting in a black powder (0.471 g, 78% yield) that was transported to the drybox and stored in the glass frit sealed from the drybox atmosphere via a rubber septum.

Crystallization was accomplished by weighing out 92 mg of the black, powdered $[Ir(1,5\text{-COD})(\mu\text{-H})]_4$ in the drybox and transferring it into a 15 mL Schlenk tube. The Schlenk tube was then sealed, removed from the drybox, and placed on a Schlenk line under Ar. Next, 2.0 mL of a room temperature *n*-pentane/THF (20:1) mixture was measured out using a gastight syringe and then added to the tube. The stopper in the Schlenk tube containing the black powder and THF was black-electrical-taped to secure it. The contents of the Schlenk tube were heated to approximately 66 °C using a heat gun, while the taped stopper was held manually to secure it during minimal boiling. The resulting solution was clear, bright-green, and homogeneous with no observable solid or particulate mass. The Schlenk tube was then placed in a −20 °C freezer. Black crystals of $[Ir(1,5\text{-COD})(\mu\text{-H})]_4$ were obtained in the tube after 4 h at −20 °C. At the end of 4 h, the Schlenk tube containing the crystals was connected to a Schlenk line, and the liquid portion was removed using a cannula. The tube containing black $[Ir(1,5\text{-COD})(\mu\text{-H})]_4$ crystals

dx.doi.org/10.1021/ic2026494 | *Inorg. Chem.* 2012, 51, 3186−3193

Scheme 2. Balanced Reaction Stoichiometry and Reaction Conditions of the Successful Synthesis of $[Ir(1,5\text{-COD})(\mu\text{-H})]_4$

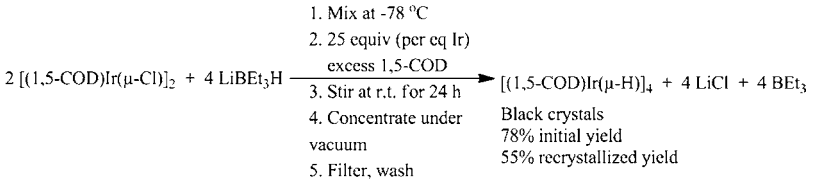

(64 mg, 55% overall yield) was kept under vacuum overnight. The crystalline material was then transported back into the drybox and stored in a 2 mL vial. The $[Ir(1,5\text{-COD})(\mu\text{-H})]_4$ complex is air-stable in crystalline form. Anal. Calcd for $C_{32}H_{52}Ir_4$ (mol wt 1205.64 g/mol): C, 31.88; H, 4.35. Found: C, 31.74; H, 4.28. ESI-MS peaks (m/z in Da, assigned ion): 1205.2478 ($[C_{32}H_{51}Ir_4]^+$), 1507.3229 ($[C_{40}H_{66}Ir_5]^+$). UV–vis peaks (nm) in THF: 476, 626. IR bands (cm^{-1}) as a KBr pellet: 697.90, 766.66, 815.67, 859.46, 866.74, 994.42, 1072.04, 1146.95, 1167.72, 1203.64, 1233.36, 1295.73, 1320.87, 1423.13, 1437.37, 1469.38, 2818.14, 2867.42, 2907.91, 2936.42, 2985.69. ^{1}H NMR in benzene-d_6 [δ in ppm (multiplicity, number of H)]: −2.89 (s, 1), 1.37 (m, 4), 2.09 (m, 4), 4.14 (m, 4). ^{13}C NMR in benzene-d_6 (δ in ppm): 68.64, 33.29.

Instrumentation and Sample Preparation. *XRD.* Single crystals of $[(1,5\text{-COD})Ir(\mu\text{-H})]_4$ suitable for XRD analysis were grown by recrystallization from 20:1 *n*-pentane/THF using the crystallization procedure detailed above. Diffraction data were collected at 120 K on a Bruker Kappa Apex II diffractometer equipped with graphite-monochromatic Mo Kα (λ = 0.710 73 Å) radiation. A suitable single crystal of $[Ir(1,5\text{-COD})(\mu\text{-H})]_4$ was mounted on a Cryoloop in Paratone-N oil. Initial lattice parameters were determined from 452 reflections harvested from 36 frames. Cell constants and other pertinent crystallographic information are reported in Tables S3–S7 in the Supporting Information. The raw intensity data were integrated and corrected for Lorentz and polarization effects; an absorption correction was applied to the data using the program *SADABS* from the *Apex II*[16] software package. The structure was solved by direct methods and refined using the *SHELXTL*[17] software package. The non-H atoms were refined with anisotropic atomic displacement parameters. H atoms bound to C atoms were included in their idealized positions and were refined with a riding model using isotropic thermal parameters 1.2 times larger than the U_{eq} value of the atom to which they were bonded. The two unique hydride atoms of the molecular core were located straightforwardly in the difference electron-density map and were refined with isotropic atomic displacement parameters.

XAFS Spectroscopy. XAFS experiments were performed at Beamline X-19A at the National Synchrotron Light Source (NSLS) at Brookhaven National Laboratory. Energy was swept from 150 eV below to 1528 eV above the Ir L_3-edge (edge energy = 11 215 eV) for the $[Ir(1,5\text{-COD})(\mu\text{-H})]_4$ sample. The X-ray absorption coefficient was measured in transmission mode by positioning the sample between the incident and transmission beam detectors. Ir^0 black was used as a reference for the X-ray energy calibration and data alignment. The Ir^0 sample was positioned between the transmission and reference beam detectors and measured simultaneously with the main sample. The X-ray detectors were gas-filled ionization chambers. A sample solution of initially crystalline $[Ir(1,5\text{-COD})(\mu\text{-H})]_4$ was freshly synthesized at Colorado State University. The black crystal was transferred into a 5 mL glass vial in a N_2-filled Vacuum Atmospheres drybox (≤5 ppm O_2). The glass vial was then double-sealed under N_2 gas and transported to the NSLS. At the NSLS, the vial was opened in a N_2-filled MBraun glovebox and the sample was prepared by brushing a fine powder uniformly onto an adhesive tape, which was then folded several times to achieve a suitable total thickness for the measurement. Within less than 3 min from removing taple sample from the glovebox, the tape sample was transferred into an airtight cell purged with N_2 for XAFS measurements.

The data processing and analysis was performed using the *IFEFFIT* package.[18] The EXAFS analysis was done by fitting the theoretical FEFF6 signals to the experimental data in r space. Theoretical contributions included only the first (Ir–C) and second (Ir–Ir) nearest neighbors (1NN). The passive electron factor, S_0^2, was found to be 0.84 by fits to the standard Ir^0 black and then fixed for further analysis of $[Ir(1,5\text{-COD})(\mu\text{-H})]_4$. The parameters describing the electronic properties (correction to the photoelectron energy origin) and local structure environment (coordination numbers N, bond lengths R, and their mean-squared disorder parameters σ^2) around the absorbing atoms were varied during the fitting. There were a total of 13 relevant independent data points and 7 variables in the fit.

RESULTS AND DISCUSSION

Initial Controls and Attempted Syntheses Based on the Literature. Initially, to calibrate our hands, the known tetrametallic hydride $[Rh(1,5\text{-COD})(\mu\text{-H})]_4$ was synthesized by two different researchers using Muetterties' original procedure,[3a] or Bönnemann's slightly revised version[3c] of Muetterties' original procedure (see the Supporting Information for details).[19] Pleasingly, dark-red crystals of the $[Rh(1,5\text{-COD})(\mu\text{-H})]_4$ complex were obtained in a 50% yield using both procedures in our hands.[20]

Next, the obvious experiments were performed in which we attempted to prepare $[Ir(1,5\text{-COD})(\mu\text{-H})]_4$ using each of three slightly different procedures published for the $[Rh(1,5\text{-COD})(\mu\text{-H})]_4$ analogue by Bönnemann,[3c] Hampden-Smith,[3b] and Muetterties[3a] (see the Supporting Information for the details of these failed syntheses).[21] A tiny amount of dark-green powder was obtained in all three trials. The trace, dark-green, Ir-product powder, from adapting Muetterties' Rh-congener procedure to the Ir case, was characterized using ESI-MS, NMR, IR, UV–vis, and X-ray photoelectron (XPS) spectroscopies (as detailed in the Supporting Information), results that encouraged us to pursue the superior synthesis reported herein. However, the yield in each case using the adapted literature procedures was extremely low (~1%)—even though we were able to prepare the $[Rh(1,5\text{-COD})(\mu\text{-H})]_4$ congener in 50% yield (that matched the literature 50–60% yields, vide supra) *prior* to the attempted Ir-congener syntheses and as control experiments. Moreover, crystallization attempts failed using the small amounts of dark-green, Ir-product powder obtained from each of the three Muetterties, Bönnemann, and Hampden-Smith adapted syntheses. Specifically, solutions cooled slowly from room temperature to −76 °C in hexane, acetone, or ethanol or cooled from room temperature to 10 °C in cyclohexane/dichloromethane (1:1) failed to produce single crystals. In addition, dissolving the complex (0.4 mg) in pentane (0.5 mL), adding acetone (pentane:acetone = 1:1 by volume), and keeping the resultant slightly cloudy solution at −78 °C for 10 h failed to provide single crystals. (The reverse order of the solvent addition was also tried.) These initial crystallization studies were undoubtedly limited by the small amounts of Ir product available from the initial, ~1% yield

dx.doi.org/10.1021/ic2026494 | Inorg. Chem. 2012, 51, 3186–3193

syntheses. Hence, the development of a higher yield synthesis became the next order of business.

Successful Synthesis and Stoichiometry of Formation of [(1,5-COD)Ir(μ-H)]$_4$. After some trial and error, the successful synthesis of [Ir(1,5-COD)(μ-H)]$_4$ was discovered, a key of which is *the use of excess 1,5-COD* that was added based on the hypothesis that it might stabilize the product. The successful synthesis is carried out starting with THF solutions of $LiBEt_3H$[22] and [Ir(1,5-COD)(μ-Cl)]$_2$ at −78 °C (Scheme 2). Excess 1,5-COD[23] (25 equivs/1 equiv of Ir) is added slowly over 5−10 min after the main reaction and at room temperature, resulting in a solution color change from dark green to bright green (the latter being the characteristic color of solutions when the black-appearing crystals of [Ir(1,5-COD)(μ-H)]$_4$ are dissolved in THF, for example, vide infra). The resulting black powder is obtained in 78% yield. Following crystallization with a *n*-pentane/THF (20:1) solution at −20 °C, 55% yield of black, crystalline [Ir(1,5-COD)(μ-H)]$_4$ was obtained. The black, crystalline [Ir(1,5-COD)(μ-H)]$_4$ complex dissolves in THF and benzene and is also slightly soluble in diethyl ether, *n*-pentane, *n*-hexane, acetone, methanol, and acetonitrile.

Single-Crystal X-ray Crystallography Structure. The single-crystal XRD structure of [Ir(1,5-COD)(μ-H)]$_4$ and the resulting atomic numbering scheme are shown in Figure 1. The

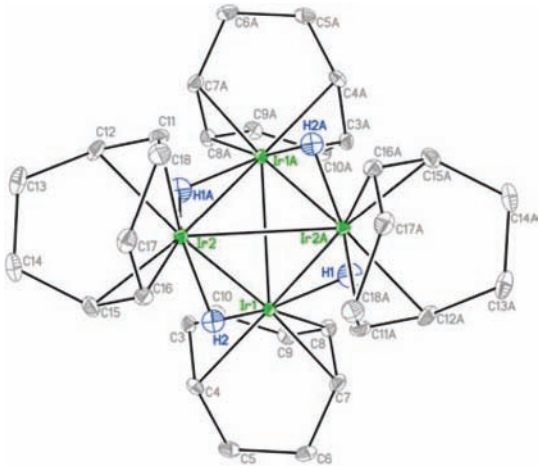

Figure 1. Single-crystal X-ray structure and atomic numbering scheme for [Ir(1,5-COD)(μ-H)]$_4$ at 50% probability.

space group is *Pbcn*, and the lattice constants are a = 12.5628(3) Å, b = 18.4647(5) Å, and c = 12.3963(3) Å. The [Ir(1,5-COD)(μ-H)]$_4$ molecule is a diamagnetic, 56-total-electron cluster, with formally 17 electrons at each Ir atom (i.e., unless one would choose to count the two *longer* Ir−Ir bonds as Ir═Ir double bonds as one way to achieve 18 electron counts at each Ir). The [Ir(1,5-COD)(μ-H)]$_4$ molecule is composed of a distorted tetrahedral Ir_4 core of D_{2d} geometry. Each Ir center is bonded to two olefinic groups of one 1,5-COD moiety plus two edge-bridging (vide infra) hydrides. The resulting Ir_4H_4 core exhibits S_4 geometry. The molecule possesses a crystallographic 2-fold symmetry (i.e., the molecule resides on a crystallographic 2-fold axis that connects the halves of the molecule, Ir1 and Ir1A, for example). Selected bond lengths and angles are given in Tables 1 and 2, respectively. Two Ir−Ir distances are long [2.90728(17) and 2.91138(17) Å] and four Ir−Ir distances are short [2.78680(12)−2.78798(12) Å].[24] A

Table 1. Selected Bond Lengths (Å) in a [Ir(1,5-COD)(μ-H)]$_4$ Crystal Obtained by XRD Structural Refinement

bond	bond length	bond	bond length
Ir1−Ir2	2.78680(12)	Ir1−C7	2.116(2)
Ir1−Ir2A	2.78798(12)	Ir1−C8	2.156(2)
Ir2−Ir1A	2.78797(12)	Ir2−C11	2.155(2)
Ir1−Ir1A	2.90728(17)	Ir2−C12	2.186(2)
Ir2−Ir2A	2.91138(17)	Ir2−C15	2.128(2)
Ir1A−Ir2A	2.78680(12)	Ir2−C16	2.158(2)
Ir1−H1	1.71(3)	C3−C4	1.407(3)
Ir1−H2	1.82(3)	C7−C8	1.424(3)
Ir2−H2	1.67(3)	C11−C12	1.405(3)
Ir1−C3	2.156(2)	C15−C16	1.419(3)
Ir1−C4	2.187(2)		

Table 2. Selected Bond Angles (deg) in a [Ir(1,5-COD)(μ-H)]$_4$ Crystal

bond	bond angle	bond	bond angle
Ir1−Ir2−Ir2A	58.537(3)	H1−Ir1−H2	108.5(15)
Ir2−Ir1−Ir1A	58.586(3)	H2−Ir2−H1A	108.2(16)
Ir2−Ir1−Ir2A	62.966(4)	C3−Ir1−C7	96.88(9)
Ir2A−Ir1−Ir1A	58.547(3)	C4−Ir1−C8	88.85(9)
Ir1−Ir2−Ir1A	62.867(4)	C11−Ir2−C15	96.77(9)
Ir1A−Ir2−Ir2A	58.497(3)	C12−Ir2−C16	87.98(9)

residual electron-density analysis strongly suggests that the hydrides are located between two Ir atoms (i.e., are edge-bridging hydrides) connected by short Ir−Ir distances. The hydride positions, from refinement of the hydride atoms using the procedure detailed in the Experimental Section, appear reasonable but may be influenced by Fourier termination errors emanating in the Ir atoms. Hence, *a neutron-diffraction experiment is needed to reveal the true positions of the hydrides* and is planned. That said, the observed short Ir−Ir distances are within the range of those of Ir−Ir bonds containing edge-bridging hydrides.[4,25] The longer Ir−Ir distances correspond to Ir−Ir bonds without bridging hydrides (Ir1−Ir1A and Ir2−Ir2A in Figure 1). These long Ir−Ir distances are slightly longer than the literature values for singly bonded Ir−Ir distances (2.65−2.73 Å).[4,2j] The observed Ir−H, Ir−C, and C−C bond distances in [Ir(1,5-COD)(μ-H)]$_4$ [1.67(3) and 1.82(3) Å, 2.116(2)−2.182(2) Å, and 1.407(3)−1.424(3) Å, respectively] are consistent with earlier literature.[4,11,26] The Ir−Ir−Ir angles vary between 58.50 and 62.86°, confirming the distorted tetrahedral shape of the Ir_4 core.[27] The H−Ir−H [108.2(16)−108.5(15)°] and C−Ir−C [88.85(9)−96.88(9)°] angles are consistent with those previously reported for similar complexes.[4]

XAFS Characterization. EXAFS and XANES were collected for two reasons: first, to test whether a minor Ir_5 species, detected by ESI-MS early in the characterization of the crystalline complex (Figure S5 of the Supporting Information), was present in the *bulk sample* of the *crystalline* material (i.e., in addition to the most abundant peak expected for the Ir_4 species, vide infra). Or, as we suspected, is the ESI-MS-observed Ir_5 species actually formed during the ESI-MS process and thus an artifact of the ESI-MS? Second, EXAFS and XANES were collected on the parent [Ir(1,5-COD)(μ-H)]$_4$ complex because these spectroscopies—and, hence, the present study—are expected to be valuable in providing a baseline/background

dx.doi.org/10.1021/ic2026494 | *Inorg. Chem.* 2012, 51, 3186−3193

study for XAFS characterization of this previously unknown complex in future applications in catalysis and other areas.

Hence, a bulk sample of *crystalline* $[Ir(1,5\text{-COD})(\mu\text{-H})]_4$ was examined by EXAFS and XANES spectroscopies. The EXAFS spectrum was analyzed only in the first nearest-neighbor range. Fourier transform (FT) magnitudes of k^3-weighted Ir L_3-edge EXAFS data of the $[(1,5\text{-COD})Ir(\mu\text{-H})]_4$ complex, and its fit using Ir−Ir and Ir−C first nearest-neighbor contributions, are shown in Figure 2. Two distinct peaks (uncorrected for the photoelectron phase shift) at around 2.5 and 1.7 Å are due to the Ir−Ir and Ir−C scattering contributions, respectively. Their real-space distances are 2.80 ± 0.01 and 2.15 ± 0.01 Å for Ir−Ir and Ir−C, respectively. The Ir−Ir coordination number (N_{Ir-Ir}) of the $[(1,5\text{-COD})Ir(\mu\text{-H})]_4$ complex is 3.0 ± 1.2, as expected for an Ir_4 core. The Ir−C coordination number (N_{Ir-C}) in the $[(1,5\text{-COD})Ir(\mu\text{-H})]_4$ crystal is 4.2 ± 0.7, as expected from one COD attachment to each Ir center. The Ir−Ir and Ir−C bond distances obtained using EXAFS (2.80 ± 0.01 and 2.15 ± 0.01 Å, respectively) are consistent with those determined using XRD [2.78680(12)−2.91138(17) and 2.116(2)−2.182(2) Å, respectively]. The lack of a higher order contribution beyond the Ir−Ir scatterer at 2.80 Å attests to the homogeneity of the samples and the lack of larger Ir clusters.

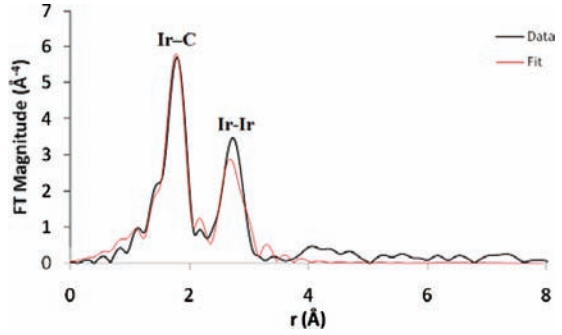

Figure 2. FT magnitudes of Ir L_3-edge EXAFS data for the $[(1,5\text{-COD})Ir(\mu\text{-H})]_4$ complex (black) and its associated fit using Ir−C and Ir−Ir contributions (red).

The XANES spectrum of $[Ir(1,5\text{-COD})(\mu\text{-H})]_4$ was obtained and compared to the XANES of both Ir^0 black and crystallographically and EXAFS-characterized[10,12] $[Ir(1,5\text{-COD})(\mu\text{-}O_2C_8H_{15})]_2$ (Figure 3). The position and height of the main absorption peak (white line) at the Ir L_3-edge are similar for $[Ir(1,5\text{-COD})(\mu\text{-H})]_4$ and Ir^0 black samples. On the other hand, the Ir L_3-edge white line is shifted to higher energy and reaches higher normalized absorption coefficient values in $[Ir(1,5\text{-COD})(\mu\text{-}O_2C_8H_{15})]_2$ compared to $[Ir(1,5\text{-COD})(\mu\text{-H})]_4$, both of which contain *formally* Ir^I. This observation indicates a higher positive charge on Ir atoms in the $[Ir(1,5\text{-COD})(\mu\text{-}O_2C_8H_{15})]_2$ complex compared to $[Ir(1,5\text{-COD})(\mu\text{-H})]_4$. Restated, the XANES-determined, "effective" oxidation state of $[(1,5\text{-COD})Ir(\mu\text{-H})]_4$ is arguably closer to that of bulk Ir^0 than the *formally* Ir^I in $[Ir(1,5\text{-COD})(\mu\text{-}O_2C_8H_{15})]_2$. However, the overall shape of the XANES spectrum (past the white line) of $[Ir(1,5\text{-COD})(\mu\text{-H})]_4$ is quite similar to that of $[Ir(1,5\text{-COD})(\mu\text{-}O_2C_8H_{15})]_2$. Both $[Ir(1,5\text{-COD})(\mu\text{-H})]_4$ and $[Ir(1,5\text{-COD})(\mu\text{-}O_2C_8H_{15})]_2$ spectra lack the post-edge oscillatory behavior seen in the bulk Ir^0 consistent with the small coordination numbers of Ir atoms in both complexes.

Additional Characterization Using ESI-MS, UV−vis, IR, and NMR. ESI-MS[28] of the black $[Ir(1,5\text{-COD})(\mu\text{-H})]_4$ crystals dissolved in dichloromethane exhibits a most abundant peak located at 1205.2478 Da (Figures S3−S5 in the Supporting Information). The experimentally observed isotopic peak distribution pattern matches the simulated isotopic distribution for $[C_{32}H_{51}Ir_4]^+$, formulated as $[Ir_4(1,5\text{-COD})_4(\mu\text{-H})_3]^+$. The UV−vis spectrum of the dark-green powder of $[Ir(1,5\text{-COD})(\mu\text{-H})]_4$ dissolved in THF shows absorption bands at 476 and 626 nm (Figure S6 in the Supporting Information). Of interest is that the experimental observation of two absorption maxima at 476 and 626 nm for $[Ir(1,5\text{-COD})(\mu\text{-H})]_4$ differ significantly from the UV−vis spectra of formally Ir^0-containing tetrairidium complexes such as $Ir_4(CO)_{11}$[*tert*-butyl-calix[4]arene$(OPr)_3(OCH_2PPh_2)$] (278 and 326 nm),[2d] or various $Ir_4(CO)_{12}$ clusters (278, 326, and 430 nm).[29] Furthermore, the UV−vis spectrum of $[Ir(1,5\text{-COD})(\mu\text{-H})]_4$ is different from that of formally Ir^I-containing $[Ir(1,5\text{-COD})(\mu\text{-}O_2C_8H_{15})]_2$ (486 nm), $[(1,5\text{-COD})Ir(\mu\text{-pyrazole})]_2$ (498 and 585 nm), and $[(1,5\text{-COD})Ir(\mu\text{-6-methyl-2-hydroxypyridine})]_2$ (484 nm).[11,30] In short, computational assistance will be required before the observed bands at 476 and 626 nm in the UV−vis spectrum of $[Ir(1,5\text{-COD})(\mu\text{-H})]_4$ in THF can be assigned with confidence.

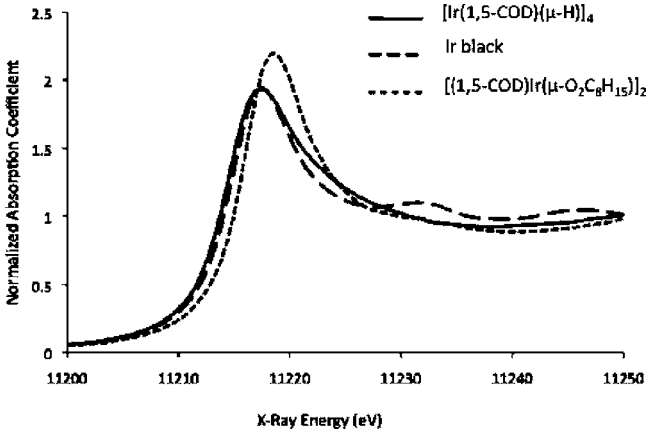

Figure 3. XANES of the $[Ir(1,5\text{-COD})(\mu\text{-H})]_4$ complex and reference compounds used of formally Ir^0 black and formally Ir^I in $[(1,5\text{-COD})Ir(\mu\text{-}O_2C_8H_{15})]_2$.[11]

The IR spectrum of the $[Ir(1,5\text{-COD})(\mu\text{-H})]_4$ complex as a KBr pellet is, as expected, similar to that of the well-characterized Rh analogue (Figure S7 in the Supporting Information).[3] The ^1H NMR spectrum of crystalline $[Ir(1,5\text{-COD})(\mu\text{-H})]_4$ dissolved in benzene-d_6 (Figure S8 in the Supporting Information) shows a signal at −2.89 ppm and has the proper integration for the four Ir−H hydrides.[31] The signals at 4.14, 2.09, and 1.37 ppm are assignable to the olefinic and methylene H atoms, respectively. The ^{13}C NMR spectrum of crystalline $[(1,5\text{-COD})Ir(\mu\text{-H})]_4$ dissolved in benzene-d_6 shows signals at 68.64 and 33.29 ppm for the COD ligands (Figure S9 in the Supporting Information), consistent with the literature values for similar Ir(1,5-COD) complexes (i.e., within the ranges of 52.6−92.6 and 27.0−33.4 ppm, respectively).[32]

Summary and Possible Future Directions. The synthesis of the previously unavailable $[Ir(1,5\text{-COD})(\mu\text{-H})]_4$ complex in 78% initial, and 55% recrystallized, yield was accomplished starting with commercially available $LiBEt_3H$ and $[Ir(1,5\text{-COD})(\mu\text{-Cl})]_2$ in the presence of excess 1,5-COD in THF. The resultant $[Ir(1,5\text{-COD})(\mu\text{-H})]_4$ was fully characterized by single-crystal XRD, XAFS, ESI-MS, UV−vis, IR, and NMR. The $[Ir(1,5\text{-COD})(\mu\text{-H})]_4$ crystal structure shows a

dx.doi.org/10.1021/ic2026494 | *Inorg. Chem.* 2012, 51, 3186−3193

distorted tetrahedral, D_{2d} Ir_4 core with one 1,5-COD and what appear to be two edge-bridging hydrides bound to each Ir center. The Ir−Ir, Ir−H, and Ir−C distances and Ir−Ir−Ir, H−Ir−H, and C−Ir−C bond angles are within the range of those for similar complexes from the extant literature. The EXAFS-determined Ir−Ir and Ir−C bond distances are in good agreement with the XRD results and validate and benchmark EXAFS as a useful method for characterization of the $[Ir(1,5\text{-}COD)(\mu\text{-}H)]_4$ complex in future applications. The EXAFS results also are of value in that they demonstrate a high degree of homogeneity of the *bulk* $[Ir(1,5\text{-}COD)(\mu\text{-}H)]_4$ sample.

As alluded to in the Introduction, there are at least five reasons why the previously unknown, tetranuclear, coordinatively unsaturated $[Ir(1,5\text{-}COD)(\mu\text{-}H)]_4$ cluster is of interest, the first of which is (i) that $[Ir(1,5\text{-}COD)(\mu\text{-}H)]_4$ holds the promise of serving as a multipurpose, coordinatively unsaturated, Ir_4-based precatalyst and organometallic synthon, analogous to its Rh congener $[Rh(1,5\text{-}COD)(\mu\text{-}H)]_4$. Our own efforts are focused on employing $[Ir(1,5\text{-}COD)(\mu\text{-}H)]_4$ (ii) as a XAFS model/standard and possible Ir_4H_4 intermediate in nucleation and growth studies of $Ir^0{}_n$ nanoclusters starting from (1,5-COD)Ir^+-based precatalysts—the role of polynuclear M_aH_b species (M metal), as opposed to just polynuclear $M^0{}_n$ species, in nanocluster nucleation and growth being an important but controversial point at present.[14,15] This new, tetrametallic cluster is also of interest (iii) as a discrete, precise composition tetrametallic Ir_4H_4 complex for possible use in the preparation of both homogeneous and supported, heterogeneous subnanometer Ir_4H_4-based catalysts, (iv) as a new precursor for testing the formation and stabilization mechanisms of Ir-based, so-called Ziegler-type industrial hydrogenation model catalysts prepared from (1,5-COD)Ir^+-based precatalysts and $AlEt_3$,[10] and (v) as a fully compositionally and structurally characterized Ir_4 analogue of the, on average, Co_4-based, subnanometer clusters identified by XAFS as a dominant species in Co-based, Ziegler-type industrial polymer hydrogenation catalysts.[15] Also noteworthy in conclusion is that the Co member of this class of tetranuclear clusters, $[M(1,5\text{-}COD)(\mu\text{-}H)]_4$ (M = Ir, Rh, Co), may be preparable as well, although it remains to be synthesized, isolated, and unequivocally characterized. Hence, it is hoped that the present synthesis and characterization, of the previously unavailable $[Ir(1,5\text{-}COD)(\mu\text{-}H)]_4$, will be of value for the above, as well as other, future studies.

■ ASSOCIATED CONTENT

Supporting Information

Instrumentation for, and the experimental procedures behind, the ESI-MS, UV−vis, IR, and NMR spectroscopic studies, literature tables for Ir−Ir bond distances and Ir−Ir−Ir bond angles of similar compounds, crystal data and structure refinement tables with bond distances, bond angles, and anisotropic and isotropic displacement parameters, a CIF file containing the crystal structure data, ESI-MS, UV−vis, IR, and NMR spectra, and detailed experimental procedures for (i) successful syntheses of $[Rh(1,5\text{-}COD)(\mu\text{-}H)]_4$, (ii) initial, low-yield-synthesis attempts for $[Ir(1,5\text{-}COD)(\mu\text{-}H)]_4$ while following literature procedures for the Rh congener, and (iii) control experiments performed to decrease the amount of a ^1H NMR-detected impurity. This material is available free of charge via the Internet at http://pubs.acs.org.

■ AUTHOR INFORMATION

Corresponding Author

*E-mail: rfinke@lamar.colostate.edu.

Notes

The authors declare no competing financial interest.

■ ACKNOWLEDGMENTS

We thank the following people working as part of the Colorado State University Central Instrumentation Facility: Stephanie Fiedler for the XRD data and Donald L. Dick for the ESI-MS data. Financial support at Colorado State University was provided by NSF Grant CHE-0611588 and at Yeshiva University by DOE BES Grant DE-FG02-03ER15476. Use of the NSLS was supported by the U.S. Department of Energy, Office of Science, Office of Basic Energy Sciences, under Contract DE-AC02-98CH10886. Beamline X19A at the NSLS is supported, in part, by the Synchrotron Catalysis Consortium, U.S. Department of Energy, Grant DE-FG02-05ER15688.

■ REFERENCES

(1) Muetterties' 1975 definition of molecular metal clusters is "discrete molecules or molecular ions that contain three or more metal atoms in a bonding interaction".[1a] Gates has commented that metal clusters are "compounds with metal−metal bonds stabilized by ligands such as carbonyls".[1b] A few lead references to the extensive literature of molecular metal clusters are given below.[1a−f] Studies comparing structure, thermochemistry, and bonding interactions in molecular metal clusters to those of bulk metal surfaces containing chemisorbed ligands have revealed that one valuable contribution of molecular metal clusters is that they can be reasonable approximations to ligated, bulk metal surfaces.[1e] (a) Muetterties, E. L. *Bull. Soc. Chim. Belg.* **1975**, *84*, 959−986. (b) Gates, B. C. *Angew. Chem., Int. Ed.* **1993**, *32*, 228−229. (c) Chini, P. *Pure Appl. Chem.* **1970**, *23*, 489−503. (d) Chini, P.; Longoni, G.; Albano, V. G. *Adv. Organomet. Chem.* **1976**, *14*, 285−344. (e) Muetterties, E. L.; Rhodin, T. N.; Band, E.; Brucker, C. F.; Pretzer, W. R. *Chem. Rev.* **1979**, *79*, 91−137. (f) Muetterties, E. L. *Science* **1977**, *196*, 839−848. (g) Chini, P. *J. Organomet. Chem.* **1980**, *200*, 37−61. (h) Calabres, J. C.; Dahl, L. F.; Cavalier, A.; Chini, P.; Longoni, G.; Martinen, S. *J. Am. Chem. Soc.* **1974**, *96*, 2616−2618. (i) Vranka, R. G.; Dahl, L. F.; Chini, P.; Chatt, J. *J. Am. Chem. Soc.* **1969**, *6*, 1574−1576. (j) Morse, M. D. *Chem. Rev.* **1986**, *86*, 1049−1109. (k) Adams, R. D. *Acc. Chem. Res.* **1983**, *16*, 67−72. (l) Adams, R. D. *Chem. Rev.* **1989**, *89*, 1703−1712. (m) Adams, R. D. *Polyhedron* **1985**, *4*, 2003−2025. (n) Adams, R. D.; Babin, J. E.; Tasi, M. *Inorg. Chem.* **1986**, *25*, 4514−4519. (o) Adams, R. D.; Chen, M. *Organometallics* **2011**, *30*, 5867−5872. (p) Adams, R. D.; Chen, M. *Organometallics* **2012**, *31*, 445−450.

(2) (a) Grunwaldt, J.-D.; Kappen, P.; Basini, L.; Clausen, B. S. *Catal. Lett.* **2002**, *78*, 13−21. (b) Li, F.; Gates, B. C. *J. Phys. Chem. B* **2004**, *108*, 11259−11264. (c) Stuntz, G. F.; Shapley, J. R.; Pierpont, C. G. *Inorg. Chem.* **1978**, *17*, 2596−2603. (d) Silva, N.; Solovyov, A.; Katz, A. *Dalton Trans.* **2010**, *39*, 2194−2197. (e) Goellner, J. F.; Guzman, J.; Gates, B. C. *J. Phys. Chem. B* **2002**, *106*, 1229−1238. (f) Li, F.; Gates, B. C. *J. Phys. Chem. B* **2003**, *107*, 11589−11596. (g) Uzun, A.; Gates, B. C. *Angew. Chem., Int. Ed.* **2008**, *47*, 9245−9248. (h) Xu, Z.; Xiao, F.-S.; Purnell, S. K.; Alexeev, O.; Kawi, S.; Deutsch, S. E.; Gates, B. C. *Nature* **1994**, *372*, 346−348. (i) Argo, A. M.; Odzak, J. F.; Lai, F. S.; Gates, B. C. *Nature* **2002**, *415*, 623−626. (j) Argo, A. M.; Odzak, J. F.; Gates, B. C. *J. Am. Chem. Soc.* **2003**, *125*, 7107−7115. (k) Uzun, A.; Gates, B. C. *J. Am. Chem. Soc.* **2009**, *131*, 15887−15894. (l) Doi, Y.; Koshizuka, K.; Keii, T. *Inorg. Chem.* **1982**, *21*, 2732−2736. (m) Doi, Y.; Koshizuka, K.; Tamura, S. *J. Mol. Catal.* **1983**, *19*, 213−222. (n) Sanchez-Delgado, R. A.; Andriollo, A.; Puga, J.; Martin, G. *Inorg. Chem.* **1987**, *26*, 1867−1870. (o) Bradley, J. S. *J. Am. Chem. Soc.* **1979**, *101*, 7419−7421. (p) Rosas, N.; Marquez, C.; Hernandez, H.; Gomez, R. *J. Mol. Catal.* **1988**, *48*, 59−67. (q) Adams, R. D.; Falloon, S. B. *Organometallics* **1995**, *14*, 4594−4600.

(3) (a) Kulzick, M.; Price, R. T.; Muetterties, E. L.; Day, V. W. *Organometallics* **1982**, *1*, 1256−1258. (b) Duan, Z.; Hampden-Smith, M. J.; Sylwester, A. P. *Chem. Mater.* **1992**, *4*, 1146−1148. (c) Bönnemann, H.; Brijoux, W.; Brinkmann, R.; Dinjus, E.; Fretzen, R.; Joußen, T.; Korall., B. *J. Mol. Catal.* **1992**, *74*, 323−333.
(4) Garlaschelli, L.; Greco, F.; Peli, G.; Manassero, M.; Sansoni, M.; Gobetto, R.; Salassa, L.; Pergola, R. D. *Eur. J. Inorg. Chem.* **2003**, 2108−2112.
(5) Cabeza, J. A.; Nutton, A.; Mann, B. E.; Brevard, C.; Maitlis, P. M. *Inorg. Chim. Acta* **1986**, *115*, L47−L48.
(6) Huttner, G.; Lorenz, H. *Chem. Ber.* **1975**, *108*, 973.
(7) Bau, R.; Ho, N. N.; Schneider, J. J.; Mason, S. A.; McIntyre, G. J. *Inorg. Chem.* **2004**, *43*, 555−558.
(8) (a) Day, V. W.; Fredrich, M. F.; Reddy, G. S.; Sivak, A. J.; Pretzer, W. R.; Muetterties, E. L. *J. Am. Chem. Soc.* **1977**, *99*, 8091−8093. (b) Brown, R. K.; Williams, J. M.; Sivak, A. J.; Muetterties, E. L. *Inorg. Chem.* **1980**, *19*, 370−374. (c) Ricci, J. S.; Koetzle, T. F.; Goodfellow, R. J.; Espinet, P.; Maitlis, P. M. *Inorg. Chem.* **1984**, *23*, 1828−1831.
(9) The tetrarhodium complex $[Rh(1,5\text{-COD})(\mu\text{-H})]_4$ has also been tested as a precatalyst for toluene hydrogenation after adsorbing it onto silica or onto palladium supported on silica.[9a] The hydrogenation of carbon dioxide began with $[Rh(1,5\text{-COD})(\mu\text{-H})]_4$ and employed $Ph_2P(CH_2)_4PPh_2$.[9b,c] (a) Stanger, K. J.; Tang, Y.; Anderegg, J.; Angelici, R. J. *J. Mol. Catal. A: Chem.* **2003**, *202*, 147−161. (b) Gassner, F.; Dinjus, E.; Grls, H.; Leitner, W. *Organometallics* **1996**, *15*, 2078−2082. (c) Leitner, W.; Dinjus, E.; Gassner, F. *J. Organomet. Chem.* **1994**, *475*, 257−266.
(10) Alley, W. M.; Hamdemir, I. K.; Wang, Q.; Frenkel, A.; Li, L.; Yang, J. C.; Menard, L. D.; Nuzzo, R. G.; Özkar, S.; Johnson, K. A.; Finke, R. G. *Inorg. Chem.* **2010**, *49*, 8131−8147.
(11) Alley, W. M.; Girard, C. W.; Özkar, S.; Finke, R. G. *Inorg. Chem.* **2009**, *48*, 1114−1121.
(12) By definition, Ziegler-type hydrogenation catalysts are formed from a non-zero-valent group 8−10 transition-metal precatalyst such as $[Ir(1,5\text{-COD})(\mu\text{-}O_2C_8H_{15})]_2$ plus a trialkylaluminum cocatalyst such as $AlEt_3$. For a review of the ∼50-year-old literature on Ziegler-type hydrogenation catalysts, see: Alley, W. M.; Hamdemir, I. K.; Johnson, K. A.; Finke, R. G. *J. Mol. Catal. A: Chem.* **2010**, *315*, 1−27.
(13) Johnson, K. A. *Polym. Prepr.* **2000**, *41*, 1525−1526.
(14) (a) Mondloch, J. E.; Finke, R. G. *J. Am. Chem. Soc.* **2011**, *133*, 7744−7756. (b) Mondloch, J. E.; Wang, Q.; Frenkel, A. I.; Finke, R. G. *J. Am. Chem. Soc.* **2010**, *132*, 9701−9714. (c) Bayram, E.; Zahmakiran, M.; Özkar, S.; Finke, R. G. *Langmuir* **2010**, *26*, 12455−12464. (d) Watzky, M. A.; Finney, E. E.; Finke, R. G. *J. Am. Chem. Soc.* **2008**, *130*, 11959−11969. (e) Ott, L. S.; Finke, R. G. *J. Nanosci. Nanotechnol.* **2008**, *8*, 1551−1556. (f) Ott, L. S.; Campbell, S.; Seddon, K. R.; Finke, R. G. *Inorg. Chem.* **2007**, *46*, 10335−10344. (g) Özkar, S.; Finke, R. G. *J. Organomet. Chem.* **2004**, *689*, 493−501.
(15) Alley, W. M.; Hamdemir, I. K.; Wang, Q.; Frenkel, A.; Li, L.; Yang, J. C.; Menard, L. D.; Nuzzo, R. G.; Özkar, S.; Yih, K. H.; Johnson, K. A.; Finke, R. G. *Langmuir* **2011**, *27*, 6279−6294.
(16) *SADABS*; Bruker Analytical X-Ray System, Inc.: Madison, WI, 1999.
(17) (a) Sheldrick, G. M., *SHELXTL*,, version 6.14; Bruker Analytical X-Ray Systems, Inc.: Madison, WI, 1999. (b) A short history of SHELX″: Sheldrick, G. M. *Acta Crystallogr.* **2008**, *A64*, 112−122.
(18) Newville, M. *J. Synchrotron Radiat.* **2001**, *8*, 322−324.
(19) Three main differences between Muetterties' original procedure and Bönnemann's synthesis are as follows: (i) Muetterties' procedure starts with 0.02 mmol of $[Rh(1,5\text{-COD})(\mu\text{-Cl})]_2$ versus 12.2 mmol in Bönnemann's synthesis; (ii) Muetterties and co-workers started with $K[HB(O\text{-}i\text{-}C_3H_7)_3]$ in THF or EtLi in toluene, whereas the hydride source in Bönnemann's synthesis is $Na[BEt_3H]$; (iii) the initial $[Rh(1,5\text{-COD})(\mu\text{-Cl})]_2$ and hydride source are mixed immediately at −78 °C in Muetterties' original synthesis versus over 9 h at room temperature in Bönnemann's synthesis.[3a,c]
(20) Muetterties' original $[Rh(1,5\text{-COD})(\mu\text{-H})]_4$ synthesis[3a] reports 50−60% yield when starting with 0.02 mmol of $[Rh(1,5\text{-COD})(\mu\text{-Cl})]_2$. We have obtained a similar yield (∼50%) using the same procedure but when starting with 1.49 mmol of $[Rh(1,5\text{-COD})(\mu\text{-Cl})]_2$. However, using Bönnemann's procedure,[3c] we obtain a lower yield (∼50%) than those reported by workers (74%), although our scale of starting with 2 mmol of $[Rh(1,5\text{-COD})(\mu\text{-H}]_4$ (vs 12.2 mmol in Bönnemann's study) is one likely reason for our somewhat lower yield in that synthesis done purely as a control reaction.
(21) Hampden-Smith and co-workers[3b] synthesized $[Rh(1,5\text{-COD})(\mu\text{-H})]_4$ by mixing 1 mmol of $[Rh(1,5\text{-COD})(\mu\text{-Cl})]_2$ and 2 mmol of $LiBEt_3H$ at 0 °C and obtained a 52% yield. See this reference, as well as ref 20, for a comparison to Muetterties' and Bönnemann's syntheses.
(22) The hydride sources $K[HB(O\text{-}i\text{-}Pr)_3]$ or EtLi used by Muetterties and co-workers[3a] were replaced by $LiBEt_3H$ in our study because of the commercial unavailability of $K[HB(O\text{-}i\text{-}Pr)_3]$ and because Hampden-Smith and co-workers successfully used $LiBEt_3H$ in their $[Rh(1,5\text{-COD})(\mu\text{-H})]_4$ synthesis.[3b] An attempted synthesis using EtLi was also performed as part of the present work but failed, as detailed in the Supporting Information.
(23) (a) The addition of free 1,5-COD is one key step that differs from Muetterties' original synthesis and which results in a ∼78-fold higher yield synthesis of $[Ir(1,5\text{-COD})(\mu\text{-H})]_4$. Another key difference from Muetterties' original synthesis is that dark green $[Ir(1,5\text{-COD})(\mu\text{-H})]_4$ is kept in a THF solution until the filtration step (whereas Muetterties' synthesis of the Rh congener evaporates the volatiles under vacuum and then extracts $[Rh(1,5\text{-COD})(\mu\text{-H})]_4$ using pentane). (b) Additionally, an impurity detectable as a 12.82 ppm peak in the ^1H NMR is present in the black powder. That impurity can be reduced by (i) washing the black powder with larger amounts of deoxygenated acetone in a drybox (a total of 250 mL vs 15 mL), (ii) increasing the stirring time from the initial 30 min to 24 h after the addition of excess 1,5-COD, or (iii) passing a concentrated $[(Ir(1,5\text{-COD})(\mu\text{-H})]_4$ solution in THF through a glass filter (i.e., without the addition of acetone). See the Experimental section of the Supporting Information for further details and the ^1H NMR spectra (Figures S1 and S2 in the Supporting Information).
(24) Similar to what has been found for $[Ir(1,5\text{-COD})(\mu\text{-H})]_4$, four short and two long M−M bonds are observed in the crystal structure of the Rh analogue. The four short bonds [2.802 (0.001) Å] were assigned to bridging hydride Rh−H−Rh groups,[3a] consistent in a general way with the prior literature in which Rh−Rh bond distances varying between 2.610 (0.005) and 2.856 (0.008) Å have been assigned to Rh−H−Rh groups.[9a,b] On the other hand, the long Rh−Rh distances in $[Rh(1,5\text{-COD})(\mu\text{-H})]_4$ of 2.971 (0.001) Å are longer than the literature values of either singly bonded Rh−Rh (2.62−2.80 Å[9b]) or Rh−H−Rh distances. (a) Brown, R. K.; Williams, J. M.; Sivak, A. J.; Pretzer, W. R.; Muetterties, E. L. *Inorg. Chem.* **1980**, *19*, 370−374. (b) Day, V. W.; Fredrich, M. F.; Reddy, G. S.; Sivak, A. J.; Pretzer, W. R.; Muetterties, E. L. *J. Am. Chem. Soc.* **1977**, *99*, 8091−8093.
(25) The Ir−Ir bond distances for Ir−H−Ir linkages in Ir_n (n = 2−4) complexes of between 2.703 and 3.290 Å have been reported: (a) Heinekey, D. M.; Fine, D. A.; Barnhart, D. *Organometallics* **1997**, *16*, 2530−2538. (b) Fujita, K.; Nakaguma, H.; Hanasaka, F.; Yamaguchi, R. *Organometallics* **2002**, *21*, 3479−3757. (c) Bau, R.; Chiang, M. Y.; Wel, C. Y.; Garlaschelli, L.; Martinengo, S.; Koetzle, T. F. *Inorg. Chem.* **1984**, *23*, 4758.
(26) The Ir−C distances in $[Ir(1,5\text{-COD})(\mu\text{-H})]_4$ are similar to the Ir−diene distances reported for[26a] $[Ir_4(CO)_5(C_8H_{12})(C_8H_{10})]$ (2.10−2.24 Å) and to those previously observed in[11] $[(1,5\text{-COD})Ir(\mu\text{-}O_2C_8H_{15})]_2$. (a) Stuntz, G. F.; Shapley, J. R.; Pierpont, C. G. *Inorg. Chem.* **1978**, *17*, 2596−2603.
(27) Similar M−M−M angles [54.93(11) and 62.53(5) Å] have been seen previously for[27a] $[(C_5Me_5)Rh(\mu_3\text{-H})]_4^{2+}$. Table S2 in the Supporting Information contains a comparison of M−M−M bond angles of tetrahedral and butterfly-shaped M_4 complexes.[8c]
(28) Many Ir_4 complexes such as $[Ir_4(CO)_5(C_8H_{12})_2(C_8H_{10})]$, $[Ir_4H_{10}(PCy_3)_4(C_9H_{11}N)_2](PF_6)_2$, $[(\eta^5\text{-}C_5Me_5)IrH]_4(BF_4)_2$, and *tert*-butylcalix[4]arene$(OPr)_3(OCH_2PPh_2)$-$Ir_4(CO)_{11}$ have been successfully characterized using MS. (a) Xu, Y.; Celik, M. A.; Thompson,

A. L.; Cai, H.; Yurtsever, M.; Odell, B.; Green, J. C.; Mingos, D. M. P.; Brown, J. M. *Angew. Chem., Int. Ed.* **2009**, *48*, 582−585. (b) Cabeza, J. A.; Nutton, A.; Mann, B. E.; Brevard, C.; Maitlis, P. M. *Inorg. Chim. Acta* **1986**, *115*, L47−L48.

(29) Tortorelli, L. J.; Flowers, P. A.; Harward, B. L.; Mamantov, G.; Klatt, L. N. *J. Organomet. Chem.* **1992**, *429*, 119−134.

(30) Marshall, J. L.; Stobart, S. R.; Gray, H. B. *J. Am. Chem. Soc.* **1984**, *106*, 3027−3029. (b) Rodman, G. S.; Mann, K. R. *Inorg. Chem.* **1988**, *27*, 3347−3353.

(31) For comparison, this −2.89 ppm chemical shift is considerably downfield compared, for example, to the hydride peak for $[Rh(1,5\text{-}COD)(\mu\text{-}H)]_4$ at ca. −12 ppm. It is also downfield from the hydride signals of previously synthesized tetrahydridotetrairidium complexes such as $[Ir(CO)(PPh_3)(\mu\text{-}H)H]_4$ or $[Ir(\eta\text{-}C_5Me_5)(\mu\text{-}H)]_4(BF_4)_2$ appearing between −12.84 and −18.89 ppm.[4,5] For a broader comparison, the ^{1}H NMR spectra of various complexes containing M−H−M (M: Ir−Rh or Re) face- or edge-bridging hydrides contain hydride peaks between −4.30 and −24.00 ppm.[31a−e,25a,b] Hence, although one could speculate on the origins of this downfield, the hydride chemical shift (using, for example, the Ramsey shielding/deshielding equation[31f] or trying to take into account the increased electron density on Ir suggested by XANES), we choose not to speculate in the absence of a good wave function and subsequent molecular orbital calculation for $[Ir(1,5\text{-}COD)(\mu\text{-}H)]_4$. Note here that the needed computations would best come *after* definitive location of the hydrides by neutron diffraction, studies that are planned. (a) Vaartstra, B. A.; Cowie, M. *Organometallics* **1990**, *9*, 1594−1602. (b) Hattori, T.; Matsukawa, S.; Kuwata, S.; Ishii, Y.; Hidai, M. *Chem. Commun.* **2003**, 510−511. (c) Mueting, A. M.; Boyle, P. D.; Wagner, R.; Pignolet, L. H. *Inorg. Chem.* **1988**, *27*, 271−279. (d) Fryzuk, M. D. *Organometallics* **1982**, *1*, 408−409. (e) Johnson, J. R.; Kaesz, H. D. *Inorg. Synth.* **1978**, *18*, 60−62. (f) Drago, R. S. *Physical Methods for Chemists*; Surfside Scientific Publishers: Gainesville, FL, 1977.

(32) (a) Adams, C. J.; Anderson, K. M.; Charmant, J. P. H.; Connelly, N. G.; Field, B. A.; Hallett, A. J.; Horne, M. *Dalton Trans.* **2008**, 2680−2692. (b) Brown, M. D.; Levason, W.; Reid, G.; Webster, M. *Dalton Trans.* **2006**, 4039−4046. (c) Browning, J.; Bushnell, G. W.; Dixon, K. R.; Hilts, R. W. *J. Organomet. Chem.* **1993**, *452*, 205−218. (d) Zotto, A. D.; Costella, L.; Mezzetti, A.; Rigo, P. *J. Organomet. Chem.* **1991**, *414*, 109−118.